Cyclization of Terpenoid Dicarbonitrile Polyalkenes upon Photoinduced Electron Transfer to 1,4-Dicyano-2,3,5,6-tetramethylbenzene and Other Cyanoarenes

Helmut Görner,* Klaus-Dieter Warzecha, and Martin Demuth

Max-Planck-Institut für Strahlenchemie, D-45413 Mülheim an der Ruhr, Germany

Received: June 20, 1997; In Final Form: September 10, 1997[⊗]

Photoinduced electron transfer from terpenoid polyalkenes bearing electron-withdrawing groups, i.e., 2,6-dimethyl-1,5-heptadiene-1,1-dicarbonitrile (**D1**) and its higher homologues **D2** and **D3**, as well as from 1,1′-biphenyl (BP) to 1,4-dicyano-2,3,5,6-tetramethylbenzene (**A1**), 1,4-dicyanonaphthalene (**A3**), 1-cyanonaphthalene (**A4**), and 9,10-dicyanoanthracene (**A5**), was studied in polar solvents by time-resolved UV−vis spectroscopy and conductivity. The transients observed for **A1** in deoxygenated acetonitrile in the presence of BP by laser flash photolysis with $\lambda_{exc} = 308$ nm are the radical cation of BP ($BP^{\bullet+}$, $\lambda_{max} = 380$ and 660 nm) and the radical anion of the acceptor ($A^{\bullet-}$, $\lambda_{max} = 360$ nm). Fluorescence quenching of **A1** and the formation of $BP^{\bullet+}$ depend on the BP concentration; at low [BP], triplet quenching of **A1** prevails, leading to ^{3}BP* via energy transfer. The transients for several other acceptors are characterized; for example, the radical anions of **A3** and **A5** absorb at $\lambda_{max} = 390$ and 312 nm, respectively. The rate constants for secondary electron transfer from **D*n*** ($n = 1-3$) or other donors to $BP^{\bullet+}$ were determined. Secondary electron transfer to the polyalkenes from the radical anion of **A1**, but not the other acceptors, was observed. The transient conductivity of the acceptor/BP/polyalkene systems in acetonitrile in the presence or absence of water indicates formation and disappearance of charges, in particular of protons. In addition, the effects of water and methanol on the yields for consumption of **D1** and formation of the products were studied by pulsed and continuous irradiation. A representative reaction scheme is suggested for the cyclization of the smallest polyalkene, **D1**, which, on the basis of the kinetic results, is proposed also for **D2** and **D3**. Furthermore, optimized reaction conditions for synthetic applications are discussed.

Introduction

Photoinduced electron transfer (PET) from terpenoid polyalkenes to cyanoaromatic electron acceptors (A) gives rise to mono- and polycyclic products in biomimetic fashion.[1−6] If the polyalkenes bear electron-withdrawing substituents, such as a dinitrile group, at the α-terminal site, formation of radical cations via photochemical electron transfer occurs exclusively at the remote ω-terminal double bond. Subsequent cyclization characteristically leads to products containing a five-membered ring. The typically observed 5-*exo*-*trig* ring closure as the terminating step is most likely the result of the stabilizing effect of the dinitrile group on the adjacent radical thus formed.[2−6] One representative example, i.e., the cyclization of (5*E*,9*E*)-2,6,10,14-tetramethylpentadeca-1,5,9,13-tetraene-1,1-dicarbonitrile (**D3**), is depicted in Scheme 1. The transformations of the homologues **D1** and **D2** have also been investigated (Chart 1).[2−6]

The role of radical ions in the photooxidation of unsaturated compounds has been the subject of intensive studies.[7−31] The singlet states of cyanoaromatics are used in this connection as efficient electron acceptors upon irradiation with UV light; the most widely employed acceptors are 1,4-dicyanobenzene (**A2**)[8,13,18,28,29] and 9,10-dicyanoanthracene(**A5**).[9−12,14−16,19−27,30,31] In the presence of an electron donor (D) in a polar solvent, the quantum yield and lifetime of ^{1}A* fluorescence decrease, as expected for an electron-transfer quenching mechanism (2a).

$$A + h\nu \rightarrow {}^1A^* \rightarrow A + h\nu' \quad (1)$$

$$^1A^* + D \rightarrow {}^1(A^* \cdots D) \rightarrow (A^{\bullet-} \cdots D^{\bullet+}) \rightarrow A^{\bullet-} + D^{\bullet+} \quad (2a)$$

SCHEME 1:

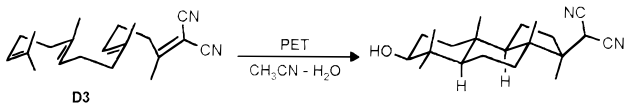

CHART 1:

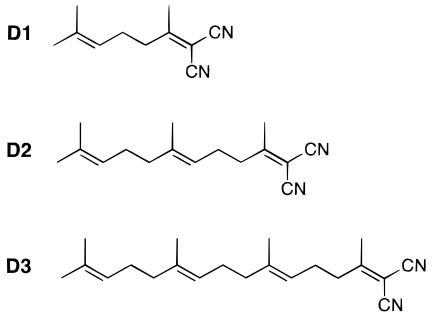

Thus, the reactive state of **A2** or **A5** is the excited singlet state (^{1}A*), although a triplet reaction after intersystem crossing from the complex ^{1}(A* ⋯ D) can generally not be excluded.[8,25]

Additives such as 1,1′-biphenyl (BP) or phenanthrene have been shown to enhance the yield of oxidation products in several cases.[2,14,15,17−22,29] The role of BP as a cosensitizer, acting as "a catalyst" and improving charge separation, can be described by reactions 2b and 3.

$$^1A^* + BP \rightarrow \rightarrow A^{\bullet-} + BP^{\bullet+} \quad (2b)$$

$$BP^{\bullet+} + D \rightarrow BP + D^{\bullet+} \quad (3)$$

Initially, electron transfer from BP to the excited acceptor forms the acceptor radical anion ($A^{\bullet-}$) and the radical cation of

[⊗] Abstract published in *Advance ACS Abstracts,* December 1, 1997.

S1089-5639(97)02027-6 CCC: $14.00

CHART 2:

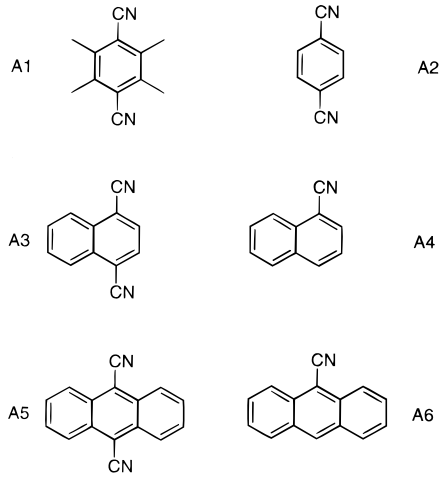

the cosensitizer ($BP^{\bullet+}$). Subsequent electron transfer from D to $BP^{\bullet+}$ regenerates BP (the rate constant is k_3; generally k_n refers to eq *n*) and yields $D^{\bullet+}$. The advantage of this cosensitizer is 2-fold. First, since BP does not absorb at wavelengths longer than 300 nm, it can be added in high concentrations, which are required for efficient fluorescence quenching. Thus, the acceptor is selectively excited with $\lambda_{exc} > 300$ nm. Second, due to the much longer half-life of $BP^{\bullet+}$ as compared to the lifetime (τ_s) of the $^1A^*$ state, the concentration of the donor, selected for synthesis, can be much lower. Thus, direct excitation of D is minimized and possible competing reactions are suppressed. The spectral and kinetic properties of $BP^{\bullet+}$ and its reactivity with various electron donors are not well documented. Open questions concern the electron transfer from radical anions to $BP^{\bullet+}$ and the influence of solvent polarity, as well as the optimum reactant concentrations required for preparative applications. BP as the cosensitizer has also been employed for cyclization processes of isoprenoid polyalkenes **D*n*** ($n = 1-3$).[2,3] The photoproducts in the presence of methanol and water are cycloalkyl methyl ethers and cycloalkanols, respectively.[1−6] Recently, photoinduced electron transfer from **D1** and derivatives thereof to 2,4,6-triphenylpyrylium tetrafluoroborate ($P^+BF_4^-$) has been examined.[4]

In the present work, photoinduced electron transfer from various donors to cyanoarenes was studied in polar solvents by time-resolved spectroscopy and conductivity using laser flash photolysis with $\lambda_{exc} = 308$ and 353 nm. The electron donors are the three 1,1-dicarbonitrile polyalkenes, and the acceptors are 1,4-dicyano-2,3,5,6-tetramethylbenzene (**A1**), 1,4-dicyanonaphthalene (**A3**), 1-cyanonaphthalene (**A4**), **A5**, and 9-cyanoanthracene (**A6**). The spectral and kinetic properties of the radical cations and anions involved are examined, allowing a more detailed mechanistic interpretation of such synthetically useful cyclization processes.

Experimental Section

The polyalkenes 2,6-dimethyl-1,5-heptadiene-1,1-dicarbonitrile (**D1**), (5*E*)-2,6,10-trimethyl-1,5,9-undecatriene-1,1-dicarbonitrile (**D2**), and **D3** were prepared as described previously.[2] For preparation of **A1**, see ref 2; **A3** was prepared from 1,4-dibromonaphthalene according to the same procedure; **A2** (Merck), **A4** (Aldrich), **A5** (Kodak), **A6** (Aldrich), BP (Fluka), acetophenone (Fluka), and 1,4-diazabicyclo[2.2.2]octane (DABCO, Aldrich) were used as received; *N*,*N*-dimethylaniline (DMA) was purified by distillation. The solvents were used as commercially available (Merck), e.g., acetonitrile (Uvasol), toluene, and dichloromethane, or purified by distillation, 2,2,2-trifluoroethanol (TFE, Aldrich) and methanol; water was purified by a Millipore (Milli Q) system.

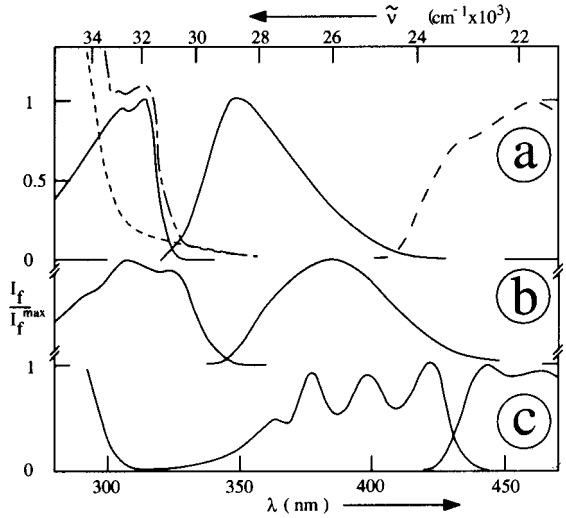

Figure 1. Absorption and fluorescence spectra in acetonitrile of (a) **A1** (full lines), (b) **A3**, and (c) **A5**; (a) absorption spectrum of **D1** (2 mM; - - -) and both **A1** and **D1** (-·-·-); phosphorescence spectrum of **A1** in ethanol at −196 °C (right curve).

The emission properties were studied with a Perkin-Elmer fluorimeter (LS-5) or a Spex-Fluorolog and a single-photon-counting apparatus[4,32] by standard procedures. The rate constant for quenching of the fluorescence lifetime by oxygen (k_{ox}) was obtained from the slope of $1/\tau_s$ vs the oxygen concentration, using τ_s values in argon-, air-, and oxygen-saturated solution. Quenching of the fluorescence intensity of **A2** by BP, due to overlap of the absorption spectra of both, is not possible. A complication arises for the fluorescence quenching of **A1** or **A3** by **D*n*** ($n = 1-3$) due to the absorption of the latter in the 300−380 nm range and the necessity to excite the acceptor at 320 nm or shorter. Therefore, the determination of the Stern−Volmer constant and the rate constant k_2 is difficult under the given conditions. The ground-state absorption spectra of **D1** and **A1** in acetonitrile are shown in Figure 1a. The molar absorption coefficients of **D1** are $\epsilon_{228} = 1.05 \times 10^4\ M^{-1}\ cm^{-1}$,[4] and $\epsilon_{312} \approx 10\ M^{-1}\ cm^{-1}$, corresponding to a **D1** concentration of ≈10 mM for equal absorption of **D1** and **A1** at 310−320 nm. Quenching measurements are therefore limited to **D*n*** concentrations ($n = 1-3$) of less than 10 mM.

The laser photolysis setup with 10−20 ns pulses was the same as described previously;[32,33] for most measurements $\lambda_{exc} = 308$ nm was used and in some cases, e.g.,for excitation measurements of **A2**, $\lambda_{exc} = 248$ nm was chosen. Excitation of **A5** was mainly carried out with $\lambda_{exc} = 353$ nm from a Nd:YAG laser. Two transient digitizers (Tektronix 7912AD and 390AD) were used; the time-resolved absorption spectra with more than 2 orders of magnitude differences were compiled from those using both short and long time ranges. Note that intense fluorescence makes observation of an absorption (e.g., of $A^{\bullet-}$ within 0.5 μs) in the relevant spectral range impossible for saturation with oxygen under our conditions. Concerning second-order decay kinetics, $t_{1/2}$ refers generally to the first half-life. The conductivity cell (internal width 0.4 cm) contained three glassy carbon electrodes (diameter 0.2 cm, distance 1.0 cm).[33] The acceptor concentrations were adjusted using absorbances of 0.5−5 at λ_{exc} (1 cm path length).

GC analysis was performed with a 15 m column (OV-1701 FS 372) on a chromatograph (Hewlett-Packard 5890) using H_2 as carrier gas. Continuous irradiation at 366 and 313 nm was performed with a 150 W mercury lamp combined with an

TABLE 1: Reduction Potential, Singlet-State Lifetime of Aromatic Nitriles, and Rate Constant for Quenching[a]

acceptor	solvent	E^*_{red} (V)	τ_s[b] (ns)	k_2 (M^{-1} s^{-1} × 10^9) BP	D3	D1
A1	acetonitrile/water[c]			11		
	acetonitrile	1.91	6.3	13	≈8	*d*
	methanol		6.0	6		
	dichloromethane			<1		
A3	acetonitrile	2.17	10.1	14		14
A4	acetonitrile	1.90	8.9	12		15
A5	acetonitrile/water[c]				14	≤4
	acetonitrile	1.97	15.3	3	10	2
A6	acetonitrile	1.40	17.2	<0.2		

[a] In argon-saturated solution, λ_{exc} = 315, 330, and 410 nm for **A*m***, m = 1, 3,4, and 5,6, respectively. [b] Taken from refs 8, 9, 12, 20 (except for **A1**). [c] $[H_2O]$ = 10 M. [d] Not possible under steady-state conditions; see text.

interference filter and a 1000 W xenon−mercury lamp combined with a monochromator, respectively. The samples were freshly prepared and the measurements were carried out at room temperature under argon unless indicated otherwise.

Results and Discussion

Fluorescence Properties. The absorption and fluorescence spectra of **A1** in acetonitrile are shown in Figure 1a. The absorption band extends to 330 nm and the energy of the singlet state is about 85 kcal mol^{-1}, in agreement with the fluorescence maximum at 350 nm. In argon-saturated acetonitrile τ_s = 6.3 ns and the rate constant for quenching by oxygen is k_{ox} = 1.5 × 10^{10} M^{-1} s^{-1}. Similar values were measured in methanol, τ_s = 6.0 ns and k_{ox}= 1.6 × 10^{10} M^{-1} s^{-1}. The fluorescence properties of **A1** and **A2** are similar. However, **A2** cannot be used for irradiation at 300 nm or above, due to its too low absorption coefficient. The absorption and fluorescence spectra of **A3** and **A5** are slightly and strongly red-shifted, respectively (Figure 1b,c). The τ_s values in acetonitrile are 9.7 ns for **A2** and 6−17 ns for the other acceptors (Table 1).

Fluorescence Quenching. Linear Stern−Volmer plots for quenching of **A1** fluorescence were obtained in acetonitrile with several donors using λ_{exc} = 315 nm. From the slopes (K_{SV}), the half-concentrations ($[D]_{1/2} = 1/K_{SV}$) and rate constants ($k_2 = K_{SV}/\tau_s$) for fluorescence quenching were determined. With BP K_{SV} = 80 M^{-1}, corresponding to k_2 =1.3 × 10^{10} M^{-1} s^{-1}. Fluorescence quenching data for several acceptors in polar solvents are compiled in Table 1. With **A5**, due to λ_{exc} = 410 nm, there is no spectral restriction for quenching by **D1** in contrast to **A1** (see Experimental Section).

Transient Absorption of A1 in the Presence of BP. The transient absorption spectra of **A1** in acetonitrile in the presence of BP are shown in Figure 2. Virtually no transient is observed between 320 and 700 nm in the absence of BP. At low BP concentrations (0.1−1 mM), a single absorption band with a maximum at 360 nm was found (Figure 2a). Following decay of the fluorescence signal, i.e., ≈0.5 μs after the 308 nm pulse, the transient at 360 nm reaches its maximum value. The decay of the 360 nm transient is mixed first- and second-order and its half-life depends on the concentration of **A1** and the laser intensity (I_L); if both [**A1**] and I_L are kept at lower values, $t_{1/2}$ approaches 10 μs. The observed species is assigned to the triplet state of BP (^{3}BP*, see below).

The transient absorption spectrum changes on further increasing the BP concentration, as shown in Figure 2b for 20 mM BP. The spectrum exhibits a major band with λ_{max} = 360 nm and a second maximum at 660 nm. At 0.3−1 μs after the 308 nm pulse the absorption at 360 nm is fully resolved. Decay of

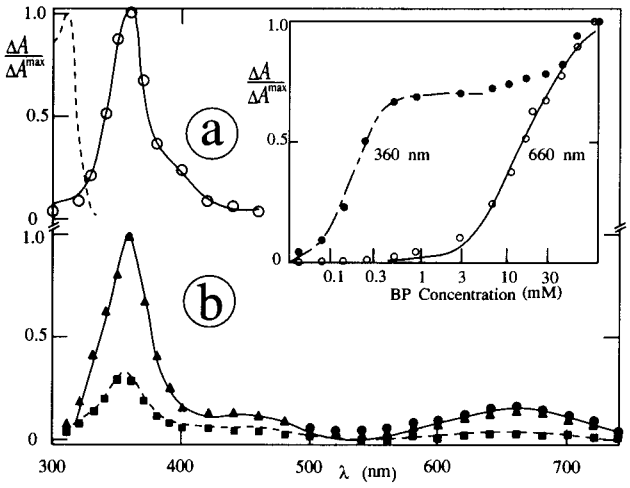

Figure 2. Transient absorption spectra of **A1** (0.5 mM) in argon-saturated acetonitrile (a) in the presence of 0.5 mM BP at 1 μs (○) after the 308 nm pulse (- - - ground state) and (b) for 20 mM BP after 0.1 μs (●), 1 μs (▲), and 5 μs (■). Inset: plots of ΔA_{360} (●) and ΔA_{660} (○) vs the BP concentration.

TABLE 2: Effects of Acceptor and Solvent on the Transient Absorption Properties[a]

acceptor	solvent	[BP] (mM)	λ_{max}[b] (nm)	$t_{1/2}$[c] (μs)	species
A1	acetonitrile/water[d]	20	*360*, 660	6/4	$A^{\bullet-}$, $BP^{\bullet+}$
	acetonitrile	0.5	360	10	^{3}BP*
		20	*360*, 660	4/2	$A^{\bullet-}$, $BP^{\bullet+}$
		200	*360*, 660	3/≤2	$A^{\bullet-}$, $BP^{\bullet+}$
		20/2[e]	*370*, 660	≤0.5	$A^{\bullet-}$, $BP^{\bullet+}$
	methanol	0.5	360	5	^{3}BP*
		20	*365*, 670	2/0.9	$A^{\bullet-}$, $BP^{\bullet+}$
	TFE	10	*360*, 660	20	$A^{\bullet-}$, $BP^{\bullet+}$
		10[f]	660	20	$BP^{\bullet+}$
	dichloromethane	20	360	2	^{3}BP*
	toluene	10−50	360	2	^{3}BP*
A3	acetonitrile	3−30	*390*, 660	5	$A^{\bullet-}$, $BP^{\bullet+}$
		30/8[e]	*390*, 660	3/0.5	$A^{\bullet-}$, $BP^{\bullet+}$
	TFE	10[f]	660	20	$BP^{\bullet+}$
A4	acetonitrile	30/10[e]	390	30	$A^{\bullet-}$
A5[g]	acetonitrile	30/10[e]	312	40	$A^{\bullet-}$
A6	acetonitrile	100	*310*, 660	3	$A^{\bullet-}$, $BP^{\bullet+}$

[a] In argon-saturated acetonitrile, [acceptor] = 0.2−1 mM, λ_{exc} = 308 nm (unless otherwise indicated). [b] Maximum italicized. [c] Longer and shorter half-lives refer to λ ≤390 and 660 nm, respectively. [d] $[H_2O]$ = 10 M. [e] Concentrations (mM) of BP/**D1**. [f] In air-saturated solution. [g] Virtually the same results using λ_{exc} = 353 nm.

the transient is essentially first-order with a second-order component, the magnitude of which depends on I_L and the wavelength of detection. Typical half-life values are $t_{1/2}$ = 4 and 2 μs at 360 and 660 nm, respectively (Table 2). The 660 nm band is assigned to $BP^{\bullet+}$,[21,34−37] whereas the UV band reflects the sum of the nonseparated absorbances from $A^{\bullet-}$ and $BP^{\bullet+}$. At even higher BP concentration (30−200 mM), the relative intensity of the signal does not change significantly. The dependences of ΔA_{360} and ΔA_{660} on the BP concentration are shown in the insets of Figure 2 for a fixed laser intensity. The peaks at 360 and 660 nm must have, at least in part, different precursors.

The transient absorption spectrum of **A1** in methanol shows a weak band at 460 nm. In the presence of BP the results are similar to those in acetonitrile in the respect that there is only the 360 nm band at small BP concentrations and there are two main bands at 360 and 660 nm (Figure 3a) at [BP] = 10−100 mM. The decay is faster at 660 nm than at 360 nm (inset of Figure 3a), and this difference is larger than in acetonitrile. Transient absorption spectra of **A1**/BP are also presented in TFE

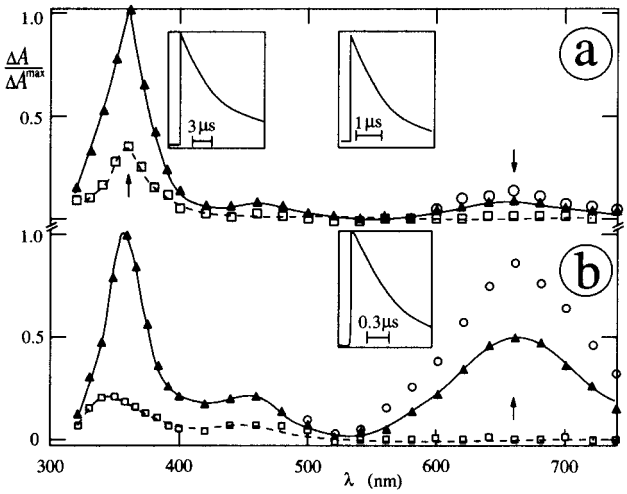

Figure 3. Transient absorption spectra in argon-saturated methanol (a) of **A1**/BP (0.5/10 mM) at 0.1 μs (○), 1 μs (▲), and 10 μs (□) after the 308 nm pulse and (b) of **A1**/BP/**D1** (0.5/30/5 mM) after 0.03 μs (○), 0.3 μs (▲), and 3 μs (□). Insets: kinetics at 360 nm (left) and 660 nm (right).

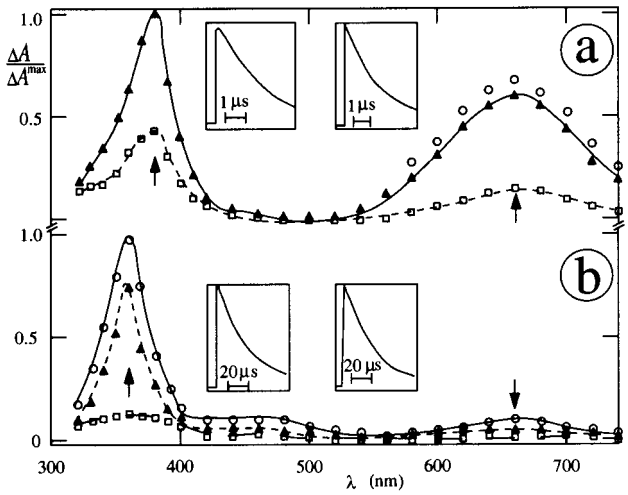

Figure 4. Transient absorption spectra of **A1**/BP (a) (0.5/30 mM) in air-saturated acetonitrile at 0.03 μs (○), 0.3 μs (▲), and 3 μs (□) after the 308 nm pulse and (b) (0.5/10 mM) in argon-saturated TFE after 1 μs (○), 10 μs (▲) and 100 μs (□). Insets: kinetics as indicated, at 360/380 nm (left) and 660 nm (right).

(Figure 4b), in methanol in the presence of **D1** (Figure 3b), and in acetonitrile/water in the presence of **D1** (Figure 5a) and **D3** (Figure 5b). Addition of water (1−20 M) to the **A1**/BP system (0.5/20 mM) in acetonitrile has no significant effect on the transient absorption spectrum. It contains two bands with maxima around 660 and 360 nm, which are again assigned to $BP^{\bullet+}$ and the sum of the absorbances from $A^{\bullet-}$ and $BP^{\bullet+}$, respectively. The decay kinetics are mixed first- and second-order, and the half-life is longer than in the absence of water (Table 2) and can slightly be enhanced by lowering I_L.

To examine the effect of solvent polarity with respect to electron or energy transfer, toluene and dichloromethane were used. The transient absorption spectrum of **A1** in toluene in the presence of BP (at low or high concentrations) is indicative for ^{3}BP* (Table 2). With **A1** in dichloromethane in the presence of BP (e.g., 10 mM), a weak transient with $\lambda_{max} \approx 340$ nm and a much stronger absorption with $\lambda_{max} = 360$ nm appear.The absence of any absorption in the 600−700 nm range clearly demonstrates that the observed transient is not $BP^{\bullet+}$. One possible explanation could be electron transfer (if the 360 nm transient would be $A^{\bullet-}$) and a too short half-life of $BP^{\bullet+}$. This,

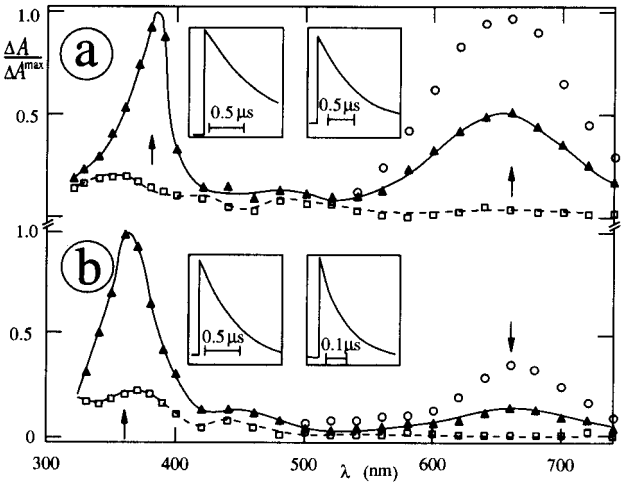

Figure 5. Transient absorption spectra of **A1**/BP (0.5/30 mM) in argon-saturated acetonitrile plus 10 M water (a) in the presence of **D1** (10 mM) at 0.03 μs (○), 0.3 μs (▲), and 3 μs (□) after the 308 nm pulse and (b) in the presence of **D3** (2 mM) after 0.02 μs (○), 0.2 μs (▲), and 2 μs (□). Insets: kinetics at 360/380 nm (left) and 660 nm (right).

however, is unlikely since $t_{1/2} \approx 20$ μs was observed for $BP^{\bullet+}$ by flash photolysis of the $P^+BF_4^-$ pyrylium salt in dichloromethane[4] or using pulse radiolysis in dichloroethane.[34] Thus we assign the 360 nm transient to ^{3}BP* and conclude that electron transfer yielding separated ions does not take place in these solvents of relatively low polarity.

Absorption of Radical Cations and Anions. For **A1** in polar solvents in the presence of oxygen and a BP concentration larger than 5 mM, the transient absorption spectrum shows again two main bands with maxima in the UV and red spectral range. However, compared to deoxygenated solution, the UV band is slightly red-shifted, and the ratio of the absorbances changes about 4-fold in favor of the 660 nm band. An example is shown in Figure 4a for air-saturated acetonitrile. This species, due to its similarity with the literature spectrum, is assigned to $BP^{\bullet+}$ alone.[34−37] The molar absorption coefficients, obtained from pulse radiolysis in aqueous solution, are $\epsilon_{380} = 1.9 \times 10^4$ and $\epsilon_{660} = 8.5 \times 10^3$ M^{-1} cm^{-1}.[37]

Radical cations are known to be rather inert toward oxygen,[38] while radical anions of aromatic molecules react with oxygen.[39]

$$A^{\bullet-} + O_2 \rightarrow A + O_2^{\bullet-} \qquad (4)$$

Whereas quenching by oxygen of the radical anions of **A1**, **A3**, **A4**, and **A5** occurs diffusion controlled, $k_4 > 1 \times 10^{10}$ M^{-1} s^{-1}, quenching of $BP^{\bullet+}$ is negligible; the rate constant is smaller than 10^8 M^{-1} s^{-1}. Generally, for **A1** in argon-saturated acetonitrile in the presence of donors other than BP, electron transfer is observed by the appearance of the 360 nm band of $A^{\bullet-}$. In certain cases, e.g., for DMA (at 460 nm), the absorption of $D^{\bullet+}$ can also be observed, depending on the ϵ value of $D^{\bullet+}$.

To generate the absorption spectrum of the acceptor radical anion, BP was replaced by DABCO, because the radical cation of DABCO has a very low molar absorption coefficient.[40] To include **A2** too, $\lambda_{exc} = 248$ nm was used. The spectra of $A^{\bullet-}$ exhibit characteristic major peaks at 360, 390, and 312 nm and minor maxima around 455, 490, and 500 nm for **A1**, **A3**, and **A5**, respectively (Figure 6). Formation of $A^{\bullet-}$ is overlapped by fluorescence and is completed after about 0.2 μs (depending on the DABCO concentration). The decay is mixed first- and second-order; the half-lives are in the 6−15 μs range throughout. Addition of 5−10 M water to **A1** and DABCO has no significant effect on the properties described above.

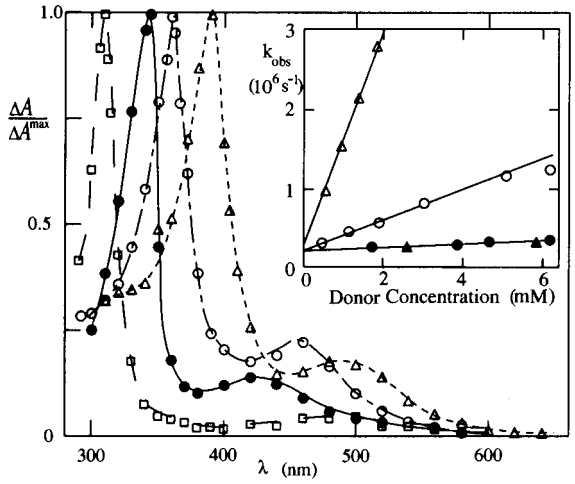

Figure 6. Absorption spectra of the radical anions in argon-saturated acetonitrile at ≈1 μs after the 248 nm pulse for **A1** (○), **A3** (△), and **A5** (□); the full circles refer to **A2** in the presence of 10 M water. Inset: rate constants for transient decay vs the donor concentration using 0.1 M BP, **A1** (0.5 mM, λ_{obs} = 360 nm, open symbols) or **A3** (0.5 mM, λ_{obs} = 390 nm, full symbols) and **D1** (circles) or **D3** (triangles); λ_{exc} = 308 nm.

SCHEME 2

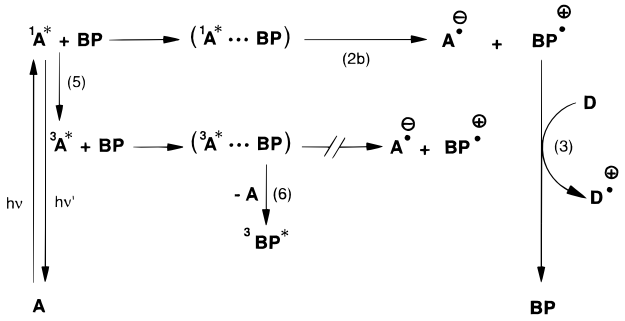

Triplet State Properties. A puzzle seems to be the appearance of the above-described 360 nm transient when trace amounts of BP (less than 1% of the half-concentration) were added to **A1** in acetonitrile in the absence of oxygen, such that fluorescence quenching is negligible (Figure 2a). We propose that the 360 nm transient originates from energy transfer of **A1** in the triplet state to BP (Scheme 2).

$$^1\mathbf{A1}^* \rightarrow {}^3\mathbf{A1}^* \qquad (5)$$

$$^3\mathbf{A1}^* + \mathrm{BP} \rightarrow \mathbf{A1} + {}^3\mathrm{BP}^* \qquad (6)$$

The assignment of the observed transient to ^{3}BP* is supported by the following: On addition of traces of oxygen, both the half-life and yield of this transient decrease. The former is due to the quenching of ^{3}BP* by oxygen, and the latter is caused by quenching of the precursor, i.e., the triplet state of **A1** (which could not be detected under our conditions). In fact, ^{3}BP* (energy: E_T = 65 kcal mol^{-1}) has its absorption maximum at 360 nm, $\epsilon_{360} = 4.0 \times 10^4$ M^{-1} cm^{-1}.[41] Also in toluene or dichloromethane at various BP concentrations ^{3}BP* but no radical ions were observed (Table 2).

In addition, energy transfer (reaction 7a) from triplet acetonaphthone (E_T = 70 kcal mol^{-1}) to BP in deoxygenated acetonitrile was studied.

$$^3\mathrm{Ketone}^* + \mathrm{BP} \rightarrow \mathrm{Ketone} + {}^3\mathrm{BP}^* \qquad (7a)$$

The resulting spectrum with λ_{exc} = 308 nm, using an appropriate BP concentration (>80% quenching), is the same as observed on direct excitation of BP at 248 nm. At −196 °C phosphorescence with λ_{max} = 450 nm was measured for **A1** in ethanol (Figure 1a); from the onset of this spectrum at ≈414 nm, E_T = 69 kcal mol^{-1} is obtained. Thus, **A1** is shown to fulfill the requirement to form ^{3}BP* by energy transfer.

To distinguish between the transient absorption spectra of the cyanoarene triplet state and the ions, energy transfer from triplet acetonaphthone to the acceptors was also examined.

$$^3\mathrm{Ketone}^* + \mathrm{A} \rightarrow \mathrm{Ketone} + {}^3\mathrm{A}^* \qquad (7b)$$

The T−T absorption maxima and the half-lives for decay of the triplet states are compiled in Table 3. The maxima are in the 420−460 nm range, except for **A1**, where no T−T absorption could be detected under our conditions. Note that the spectrum of **A5** has also a maximum at 805 nm.[23] The triplet energies of **A2**, **A4**, **A3**, and **A5** are E_T = 70.1, 57.4, 55.5, and 41.8 kcal mol^{-1}, respectively, as reported in the literature.[8,25]

TABLE 3: T−T Absorption Maximum and Triplet Lifetime of Acceptors and BP upon Direct[a] and Sensitized[b] Excitation[c]

compound	λ_{max}[a] (nm)	τ_T (μs)	λ_{max}[b] (nm)	τ_T (μs)
BP	360	10	360	10
A1	*d,e*		*d*	
A3	470	5	460	5
A4	440	10	460	5
A5	440[f]		430	5
A6			425	5

[a] [Acceptor] = 0.2−1 mM, λ_{exc} = 308 nm. [b] After energy transfer from acetonaphthone, λ_{exc}= 248 nm. [c] In argon-saturated acetonitrile. [d] No triplet observed. [e] A weak T−T absorption at 440 nm in methanol. [f] Taken from ref 25.

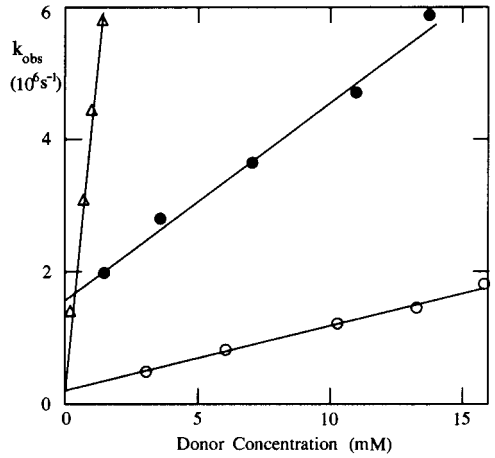

Figure 7. Plots of the rate constant for decay of the transient at 660 nm vs the donor concentration for **A1**/BP (0.5/10 mM) in argon-saturated acetonitrile (open symbols) and methanol (full symbols) using **D1** (circles) and **D3** (D).

Quenching of the Radical Cation of BP. To study the electron transfer from **D1** to BP$^{\bullet+}$, the rate constant (k_3) for decay at 660 nm vs [**D1**] was measured using the **A1**/BP system in acetonitrile. The rate constant increases linearly with the polyalkene concentration (Figure 7). From the slope the rate constant for the electron transfer from **D*n*** to BP$^{\bullet+}$ was obtained; the values range from $k_3 = 1.3 \times 10^8$ M^{-1} s^{-1} for **D1** to 2×10^{10} M^{-1} s^{-1} for DMA (Table 4). In methanol, due to the shorter half-life of BP$^{\bullet+}$ than in acetonitrile (Table 2), a larger donor concentration is necessary for sufficient quenching. On the other hand, in methanol in the presence of **D1**, k_3 is 2.2 times larger than in acetonitrile.

TABLE 4: Rate Constants for Electron Transfer from D to $BP^{\bullet+}$ (k_3) and from $A^{\bullet-}$ to D (k_{12})[a]

acceptor	solvent	donor	k_3 (10^9 M^{-1} s^{-1})	k_{12}[b] (10^9 M^{-1} s^{-1})
A1	acetonitrile	DMA	20 (0.03)[c]	<0.1
	acetonitrile/water[d]	**D1**	0.1	
	acetonitrile	**D1**	0.13 (4)	0.2
		D2	2 (0.3)	1.0
		D3	3.2 (0.16)	1.2
	methanol	**D1**	0.29	>0.2
A3	acetonitrile	**D1**	0.15 (3)	<0.05
		D3	3.4 (0.14)	<0.05
A5	acetonitrile	**D1**	0.1	

[a] In argon-saturated acetonitrile, [acceptor] = 0.2−1 mM, λ_{exc} = 308 nm; [BP] = 10−20 mM (unless otherwise indicated). [b] For sufficient fluorescence quenching [BP] = 0.1 M was used. [c] Values in parentheses refer to half-concentrations (in mM) using $t_{1/2}$ = 2 μs. [d] $[H_2O]$ = 10 M.

A significantly longer half-life of $BP^{\bullet+}$ was only measured in TFE, where the stability of radical ions is prolonged.[38,42] This indicates that the rate constant of electron back-transfer in TFE is smaller than in acetonitrile under otherwise the same conditions. Regardless of the solvent effect, the second-order ion decay should be due to reaction 8.

$$BP^{\bullet+} + A^{\bullet-} \rightarrow BP + A \qquad (8)$$

The first-order ion decay could be ascribed to a reaction involving the solvent. A reaction of $BP^{\bullet+}$ with acetonitrile is unlikely because of its relatively long half-life of 10−15 μs with a pyrylium salt as acceptor.[4] Decay of $BP^{\bullet+}$ via reaction with the solvent, however, is indicative for alcohols (eq 9) since its half-life in methanol is only 0.9 μs (Table 2); i.e., $k_9 \approx 3 \times 10^5$ M^{-1} s^{-1}.

$$BP^{\bullet+} + MeOH \rightarrow BP^{\bullet}-OMe + H^+ \qquad (9)$$

In the presence of oxygen, electron transfer to $BP^{\bullet+}$ from $O_2^{\bullet-}$ should be considered.

$$BP^{\bullet+} + O_2^{\bullet-} \rightarrow BP + O_2 \qquad (10)$$

Reaction 10, although the decay at 660 nm is not significantly faster in the presence of oxygen, is supported by conductivity measurements (see below).

An open question is the formation of the dimer radical cation.

$$BP^{\bullet+} + BP \rightarrow (BP)_2^{\bullet+} \qquad (11)$$

Such a reaction is known for other systems.[43] For BP, however, $t_{1/2}$ does not strongly decrease (<50%) with increasing the BP concentration (10−200 mM). If the spectrum of $(BP)_2^{\bullet+}$ is markedly different from that of $BP^{\bullet+}$, it can be concluded that reaction 11 does not play a role under the applied conditions. Otherwise, the reactivity of $(BP)_2^{\bullet+}$ toward **D*n*** (n = 1−3) should be comparable to that of $BP^{\bullet+}$.

Quenching of the Radical Anion of A1. So far, no reaction of $A^{\bullet-}$ with a polyalkene was expected under the above quenching conditions. However, for **A1**/BP/**D1** the transient absorption at 360 nm (due to $A^{\bullet-}$) exhibits a faster decay than in the absence of **D1**. Close inspection of the transient absorption spectra in the presence of various concentrations of **D1** reveals that the decay of $A^{\bullet-}$ becomes faster with increasing **D1** concentration. In fact, the spectrum with λ_{max} = 380 nm (Figure 5a) after fast decay of $A^{\bullet-}$ is only due to $BP^{\bullet+}$. Thus, $A^{\bullet-}$ reacts with either **D1** or a subsequent intermediate. The former process could be described by reaction 12 (Scheme 3).

SCHEME 3:

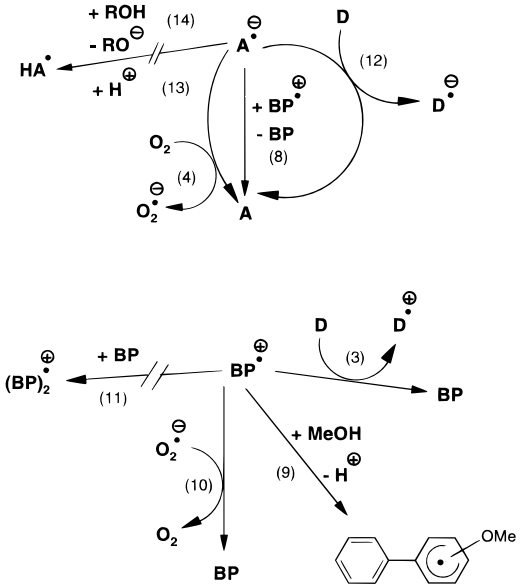

$$\mathbf{A1}^{\bullet-} + \mathbf{Dn} \rightarrow \mathbf{A1} + \mathbf{Dn}^{\bullet-} \qquad (12)$$

The rate constant (k_{12}) for decay at 360 nm vs [**D1**] using **A1**/BP (0.5/100 mM) in acetonitrile increases linearly from ≈0.3 × 10^6 s^{-1} in the absence of a second donor to 1.4 × 10^6 s^{-1} in the presence of 6 mM **D1** (inset of Figure 6). From the slope a value of $k_{12} \approx 2 \times 10^8$ M^{-1} s^{-1} for this "unexpected" electron transfer was obtained. With **D2** and **D3** a similar effect and larger k_{12} values were measured.

The transient absorption spectra for the **A1**/BP/**Dn** (n = 1, 3) systems do not significantly change in the presence of water (1−10 M). Whether the transient absorption spectrum is mainly due to $A^{\bullet-}$ or $BP^{\bullet+}$ depends on the rate constants k_3 and k_{12}. For example, if k_{12} is significantly larger than k_3, as in the case of **D1**, the intermediate species is $BP^{\bullet+}$ (Figure 5a). On the other hand, if $k_3 > k_{12}$, as in the case of **D3**, only $A^{\bullet-}$ can be observed (Figure 5b). To investigate the possibility for protonation of $A^{\bullet-}$,

$$A^{\bullet-} + H^+ \rightleftharpoons HA^{\bullet} \qquad (13)$$

the decay of $\mathbf{A1}^{\bullet-}$ was examined in argon-saturated acetonitrile in the presence of 15 M water. No discernible change in $t_{1/2}$ could be detected on addition of $HClO_4$ (up to 1 M), corresponding to $k_{13} \leq 1 \times 10^5$ M^{-1} s^{-1} (similar results were found for **A3** and **A4**). The only pK_a value available in the literature[44] (besides a pK_a ≈7 for benzonitrile[45]) is close to zero for **A2**. Also a reaction of $A^{\bullet-}$ with the solvent,

$$A^{\bullet-} + ROH \rightarrow HA^{\bullet} + RO^- \qquad (14)$$

may be excluded on the basis of longer half-lives for $A^{\bullet-}$ than for $BP^{\bullet+}$ (or nearly the same $t_{1/2}$) in several solvents (Table 2).

Electron Transfer to A3 and A5. The triplet state of the naphthalene and anthracenecyano derivatives, eventhough Φ_{isc} is larger than zero, is not dominant in absorption and plays no role as reactive state in electron transfer. The transient absorption spectra of **A3** and **A5** in acetonitrile in the presence of BP are shown in Figures 8a and 9a, respectively. The major maximum of **A3**/BP at 390 nm and of **A5**/BP at 312 nm is due to $A^{\bullet-}$ (Table 2). For **A3** the observed spectrum of $A^{\bullet-}$ is in

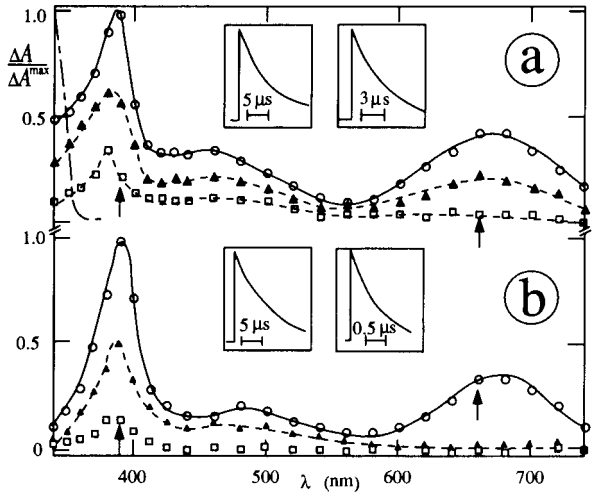

Figure 8. Transient absorption spectra of **A3**/BP (0.3/30 mM) in argon-saturated acetonitrile (a) at 0.3 μs (○), 3 μs (▲), and 10 μs (□) after the 308 nm pulse (-·-·- ground state) and (b) in the presence of **D1** (5 mM) after 0.3 μs (○), 3 μs (▲), and 30 μs (□). Insets: kinetics at 390 nm (left) and 660 nm (right).

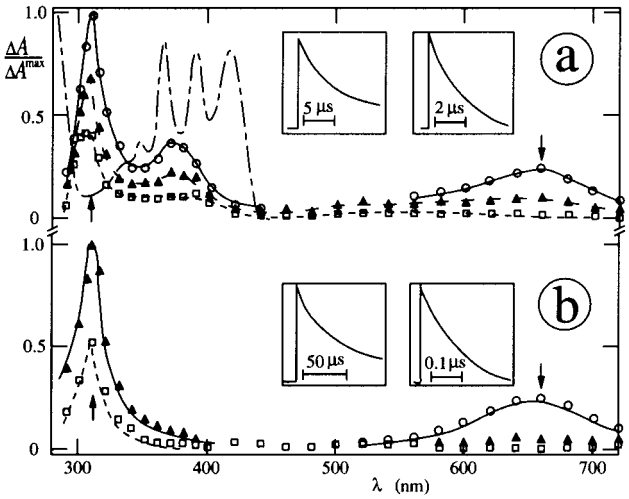

Figure 9. Transient absorption spectra of **A5**/BP (0.2/30 mM) in argon-saturated acetonitrile (a) at 0.2 μs (○), 2 μs (▲), and 20 μs (□) after the 353 nm pulse (-·-·- ground state) and (b) in the presence of **D1** (10 mM) after 0.05 μs (○), 0.5 μs (▲), and 20 μs (□). Insets: decay kinetics at 310 nm (left) and 660 nm (right).

agreement with the literature,[13] but for **A4**, **A5**, and **A6** the maxima in the UV range are presented here for the first time.

The spectrum of **A3**/BP in acetonitrile at the end of the pulse is not changed on addition of **D1** (1 mM); that is, the initial species are $A^{\bullet-}$ and $BP^{\bullet+}$. At a higher **D1** concentration (5 mM), the spectrum at >3 μs resembles that of $A^{\bullet-}$; that is, there is no new transient formed (Figure 8b). This may be interpreted by formation of $BP^{\bullet+}$ (reaction 2b) and its subsequent efficient quenching by **D1** (reaction 3). In contrast to **A1**, the radical anions of **A3** and **A5** show no reaction with **D1** (Table 4). The rate constants for reaction of $BP^{\bullet+}$ with a given donor should be independent of the nature of the acceptor. In fact, for **Dn** ($n = 1-3$) k_3 is the same (within experimental error) applying **A1** or **A3**. On addition of **D1** to **A5**/BP in acetonitrile, the spectrum is due to $A^{\bullet-}$ and $BP^{\bullet+}$ (Figure 9b). At later times, i.e., after efficient quenching of $BP^{\bullet+}$, the spectrum of $A^{\bullet-}$ remains and a component of the decay at 312 nm is significantly longer (Figure 9b, inset) than for the other acceptors.

Transient Conductivity. A conductivity increase was observed upon excitation of **A1** in acetonitrile in the presence of BP (>2 mM). The signal has its maximum ($\Delta\kappa^\circ$) at the end

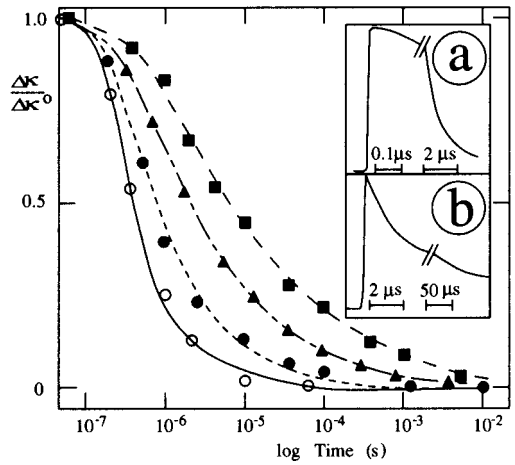

Figure 10. Conductivity signals in argon-saturated acetonitrile (open symbols) and in the presence of 10 M water (full symbols) vs time (log scale) for **A1**/BP (0.5/30 mM) (circles) and in the presence of **D1** (4 mM, triangles) or **D3** (1 mM, squares), $\lambda_{exc} = 308$ nm. Insets: kinetics (a) in the absence and (b) in the presence of **D3**.

TABLE 5: Normalized Signals of Transient Conductivity[a]

			$\Delta\kappa/\Delta\kappa^\circ$			
compound	solvent	log t	−6	−5	−4	−3
A1/BP	acetonitrile	none	0.25	0.008	0.002	0.001
		D1	0.38	0.15	0.05	0.01
A1/BP	acetonitrile/water[b]	none	0.42	0.12	0.02	0.01
		D1	0.65	0.25	0.10	0.02
		D3	0.85	0.45	0.22	0.08
A3/BP	acetonitrile	none	0.25	0.02	0.003	0.001
		D1	0.51	0.15	0.04	0.01
A3/BP	acetonitrile/water[b]	none	0.28	0.08	0.02	0.01
		D1	0.65	0.25	0.10	0.02
		D3	0.78	0.45	0.18	0.06
A5/BP	acetonitrile/water[b]	none	0.28	0.09	0.03	0.01
		D3	0.60	0.37	0.20	0.07

[a] In argon-saturated solution, [acceptor] = 1−1.8 mM, $\lambda_{exc} = 308$ nm for **A1** or **A3** and 353 nm for **A5**, [BP] = 30 mM, [donor] = 5−10 and 1−2 mM for **D1** and **D3**, respectively; $\Delta\kappa^\circ$ refers to the end of the pulse. [b] $[H_2O] = 10$ M.

of the 308 nm pulse and decreases within a few microseconds, reaching values of less than 5% of $\Delta\kappa^\circ$ (in the absence of polyalkenes) after ≈10 μs (Figure 10). The $\Delta\kappa^\circ$ value increases with the BP concentration (keeping I_L constant), thus demonstrating the prevalence of free charge formation due to electron transfer, reaction 2b. The decay of $\Delta\kappa$ is in agreement with charge annihilation via electron back-transfer, reaction 8. The contribution of a second-order decay process was proven by the ≈50% reduced half-life on 4-fold increase of I_L. On saturation with oxygen $\Delta\kappa^\circ$ is moderately lowered, in agreement with reduced electron transfer from BP to $^1A^*$ due to fluorescence quenching by oxygen with otherwise a similar decay. This supports involvement of reactions 2b, 4, and 10. The presence of 1−15 M water in acetonitrile does not change the pattern markedly. However, addition of **D1** to (aqueous) acetonitrile gives rise to a longer lived component of $\Delta\kappa$. This is illustrated in Figure 10 for the **A1**/BP/**D1** (0.5/30/4 mM) system. The results from evaluation of the conductivity decay signals of several cases are compiled in Table 5.

We have previously suggested that the cyclization of **D1** in the presence of water involves the release of a proton in an intermediate step.[1−3] To examine whether the longer lived conductivity signal results from a proton, phosphate buffer (≈0.3 mM) was added. Under these conditions, a total disappearance of the conductivity signal, apart from the first part (<2 μs), was observed. We therefore conclude that the longer lived

TABLE 6: Relative Quantum Yields for Consumption of D1 and Formation of Ethers (Φ_E) and Alcohols (Φ_A)[a]

acceptor	[additive] M	[BP] mM	$\Phi(-D)/\Phi(-D)^{max}$	$\Phi_E/\Phi(-D)^{max}$	$\Phi_A/\Phi(-D)^{max}$
methanol					
A1	0.2	10	0.55	0.1	
	1.6	10	0.8	0.2	<0.01
	1.6	40	0.8	0.3	
	1.6	140	0.8	0.4	
	1.6[b]	10	0.55	<0.01	
	8	10	0.9	0.25	
	13	10	0.7		
A3	0.2	10	0.8	0.2	
	1.6	10	0.8	0.4	<0.01
	1.6[b]	10	0.6	<0.01	
	4	10	0.7	0.3	
	10	10	0.6	0.1	
A5	0.2	3	0.4	0.1	
	0.2	9	0.95	0.3	<0.05
	0.2	30	0.9	0.2	
	1.6	10	1.0	0.5	
water					
A1	0.05	10	0.1		0.02
	0.5	10	0.4		0.15
	5	10	0.6	<0.01	0.2
	14	10	0.7		0.3
	28	10	1.0		0.5
	5[b]	10	0.45		<0.01
A3	<0.05	10	0.08	<0.02	<0.02
	0.5	10	0.5	<0.02	0.2
A5	<0.05	10	0.5		0.2
	0.2	10	0.6		0.2
	0.5[b]	10	0.4		<0.03
	1.5	10	0.9	<0.01	0.25
	5	10	0.4	<0.01	0.2

[a] Continuous irradiation in argon-saturated acetonitrile in the presence of **D1** (4.0 mM) and **A1** (0.8−8 mM) or **A3** (0.3−3 mM), $\lambda_{irr} = 313$ nm or **A5** (0.3−0.9 mM), $\lambda_{irr} = 366$ nm. [b] O_2-saturated.

conductivity signal in the absence of a buffer indeed originates in a proton (see below). An even longer lived component was found for the **A*m***/BP/**D3** ($m = 1, 3, 5$) systems (Figure 10 and Table 5). This should be the result of two additional slow 6-*endo-trig* cyclization steps prior to final 5-*exo-trig* cyclization (as for **D1**) and subsequent protonation.

Steady-State Photolysis. On irradiation of **A1** in argon-saturated acetonitrile in the presence of BP and **D1** ($\lambda_{irr} = 313$ nm), [**D1**] decreases as a function of dose, while [**A1**] remains essentially constant. From these dependences, the quantum yields for consumption of **D1**, $\Phi(-D)$, and for the formation of the alcohols (Φ_A) or ethers (Φ_E) were obtained (sum of two diastereomers). The results for the three **A*m***/BP/**D1** ($m = 1, 3, 5$) systems and various concentration ratios are compiled in Table 6. The relative $\Phi(-D)$ values in the presence of **A1** in acetonitrile and small amounts of methanol increase with the BP concentration, reach a maximum at ≈10 mM, and remain constant even up to [BP] = 140 mM. Keeping [BP] constant at 10 mM, the $\Phi(-D)$ values increase with the methanol concentration, reach a maximum at ≈8 M, and decrease slightly on going to [MeOH] = 13 M. Replacing methanol by water leads to larger $\Phi(-D)$ values with increasing water concentration, approaching a maximum value at $[H_2O] = 20-30$ M. The relative Φ_E and Φ_A values are generally substantial when $\Phi(-D)$ is large, i.e., under argon and sufficiently large BP concentration, but small in the presence of oxygen.

Similar results were obtained for **A3** and **A5**, $\lambda_{irr} = 313$ and 366 nm, respectively. The concentration of **D1** decreases as a function of dose, while **A3** or **A5** are not consumed. The photoproducts in the presence of methanol and water are likewise ethers and alcohols, respectively. For the three acceptors neither the concentrations of methanol (0.2−1.6 M) nor water (0.1−28 M) show a significant effect on $\Phi(-D)$ (Table 6). While a strong decrease of Φ_E or Φ_A was observed in the presence of oxygen throughout, the oxygen effect on $\Phi(-D)$ is relatively small.

Conditions for Synthetic Work. The choice of the acceptor is related to the wavelength of irradiation, 350−420 nm for **A5** and, if possible, 300−330 nm for **A1** and **A3**; **A2** is not suitable owing to the spectral overlap with BP. The acceptor concentration seems not to be limited by secondary reactions; note that the acceptors are fully restored; that is, they act as catalysts.[2,3] For the **A1**, **A3**, or **A5**/BP/**Dn** ($n = 1-3$) systems in polar solvents, the concentrations should be chosen as follows. [BP] should be larger than $1/K_{SV}$; appropriate values are 10−50 mM, except for **A6**, where k_2 is much lower than the diffusion-controlled limit (Table 1). The donor concentration is limited by competition of reaction 3 with the other decay routes of $BP^{\bullet+}$ and by competition of reaction 12 with the other decay routes of $A^{\bullet-}$ (Scheme 3). Concentrations of ≈5 mM for **D1** and ≈0.5 mM for **D3** are sufficient (see Table 4).

The choice of the solvent is related to the specific secondary reactions for the polyalkene which involve a nucleophilic addition and require protonation after cyclization. In this respect the $\Phi(-D)$ values in Table 6 are helpful. A high methanol concentration may reduce $\Phi(-D)$ due to competition of reactions 9 and 3; this can, in principle, be compensated by a larger donor concentration. The optimum amount of water may depend on the choice of the acceptor since for **A1** the Φ values increase with increasing the water concentration up to 20−30 M, whereas for **A5** the steady increase of the Φ values is limited to [water] ≈ 5 M.

Mechanistic Aspects. In contrast to the $P^+BF_4^-$ pyrylium salt,[4] the acceptor triplet state does not play a role in electron transfer to cyanoarenes. The yields of cyclization products are strongly enhanced by BP, which acts as a cosensitizer in a generally accepted fashion.[7,14,17−22,29] Apart from triplet energy transfer to BP (Scheme 2) and the coaccepting properties of **D*n*** ($n = 1-3$), the reaction scheme for **A3** and **A5** is suggested to be the same as for **A1** (Scheme 3). Quenching of the $^1A^*$ state by BP in a sufficiently large BP concentration is more effective than by **D1**; that is, reaction 2b is dominant.

The secondary reactions of the **D1**/**A*m*** systems ($m = 1, 3, 5$) are illustrated in Scheme 4. Cyclization in the presence of a nucleophilic solvent, such as water (R = H) or methanol (R = Me), can, in principle, occur either directly from the initial radical cation (which leads to a distonic radical cation and is followed by addition of ROH and deprotonation) or from the noncyclic **D1**•OR type radicals. In both cases, a cyclic radical ($I^\bullet$) should be formed.

$$\mathbf{D1}^{\bullet+} + \mathrm{ROH} \rightarrow \mathrm{I}^\bullet + \mathrm{H}^+ \qquad (15)$$

In view of the lifetime (≤0.1 ns)[46] of the cyclohexyl radical cation in aqueous solution (being formed by electron transfer from cyclohexene) and the previous attempt to observe $\mathbf{D1}^{\bullet+}$ in aqueous ethanol under the conditions of direct photoionization,[4] anti-Markovnikov addition of the nucleophile to $\mathbf{D1}^{\bullet+}$, followed by radical cyclization, is the most plausible reaction. Three pathways may be considered for the termination step in the absence of oxygen:

(1) H-atom transfer, for example, from a $HA^\bullet$ type radical,

$$\mathrm{HA}^\bullet + \mathrm{I}^\bullet \rightarrow \mathrm{A} + \mathrm{HI} \qquad (16)$$

(2) electron transfer from $A^{\bullet-}$

SCHEME 4:

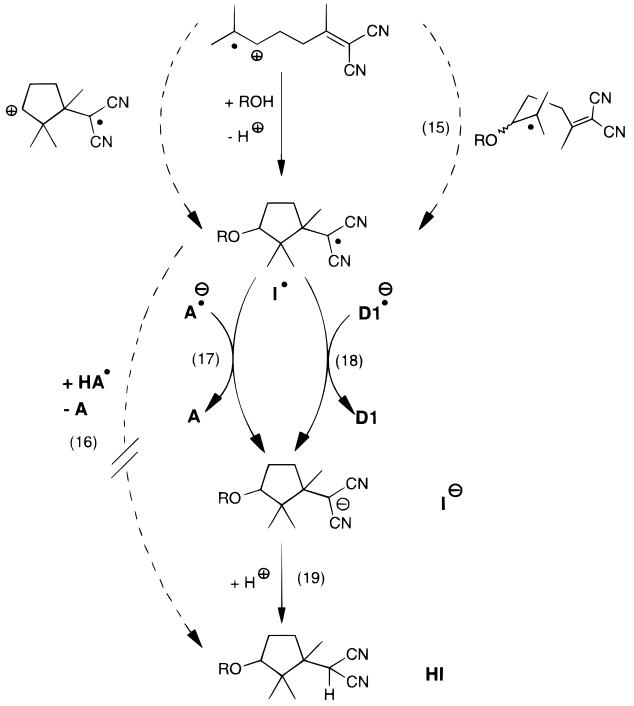

$$A^{\bullet -} + I^{\bullet} \rightarrow A + I^{-} \qquad (17)$$

or (3) electron transfer from $\mathbf{D1}^{\bullet -}$ in the case of **A1**, where reaction 12 is involved (see above).

$$\mathbf{D1}^{\bullet -} + I^{\bullet} \rightarrow \mathbf{D1} + I^{-} \qquad (18)$$

In the latter cases, the proposed intermediate is a malononitrile type anion (I^-), which, after protonation, forms the corresponding alcohols or ethers in the presence of water or methanol, respectively (Table 6).

$$I^{-} + H^{+} \rightarrow HI \qquad (19)$$

Reaction 16, however, can be excluded since formation of $HA^{\bullet}$ type radicals (**A*m***, $m = 1, 3, 5$) either via reaction 13 or 14 were not observed (see above). Reduction of $I^{\bullet}$ via reaction 17 is likely to occur for **A3**, **A4**, and **A5**. For **A1**, however, the behavior is different; the reduction of $I^{\bullet}$ occurs via reaction 18, because in the presence of **D1**, **D2**, or **D3** $\mathbf{A1}^{\bullet -}$ is rapidly replaced by $\mathbf{D}n^{\bullet -}$ (Table 4). I^- and its presursor cannot be observed by optical detection, but the fast decay of $\mathbf{A1}^{\bullet -}$ (Figure 5a,b) shows that reaction 12 is completed within a few microseconds. On the other hand, the rather long-lived conductivity signals in the presence of **D1** and more pronounced with **D3** (Figure 10 and Table 5) indicate that the cyclization steps prior to neutralization (reaction 19) require longer times.

In the general case, oxidation of the donor is irreversible in the presence of water due to rapid interception of $D^{\bullet +}$ by the nucleophile; that is, electron back-transfer may not simply restore D. Concerning the effect of oxygen, it can be suggested that there is no apparent reason for a drastical reduction of the yield of the polyalkene radical cation, apart from competition of fluorescence quenching by oxygen and formation of $BP^{\bullet +}$. A conceivable target for interception by oxygen, thereby reducing drastically the formation of the stable alcohols or ethers (Table 6), is either the noncyclic or the cyclic radicals (**D1**$-^{\bullet}$OR or $I^{\bullet}$, respectively).

Acceptor and Donor Redox Properties. The reduction potential of the acceptors in the excited singlet state (vs SCE) decreases from $E^*_{red} = 2.67$ V for **A2** to 1.40 V for **A6**.[7,16,26,47] The oxidation potential of BP is estimated to be $E_{ox} = 1.8$ V and those of the polyalkenes are ≈1.8 V for **D2** (data not shown) and **D1** and ≈1.7 V for **D3**. This is based on the k_2 values (Table 1) assuming that they follow the Rehm−Weller relationship.[48]

$$\Delta G = E_{ox} - E^*_{red} - E_c \qquad (20)$$

Here, ΔG is the free enthalpy change for electron transfer and the term E_c accounts for ion pairing (0.06 V in acetonitrile). The decrease of the oxidation potential in the order **D1**, **D2**, and **D3** is also reflected by the k_3 values for electron transfer to $BP^{\bullet +}$ (Table 4).

Concluding Remarks

In the present work, time-resolved techniques are successfully applied to characterize the accessible intermediates, to determine their reactivities, and to establish the reaction mechanism of photoinduced cyclization of isoprenoid polyalkenes. A new secondary electron-transfer reaction from the radical anion of **A1** to the polyalkenes is suggested. On the basis of the reaction kinetics the optimum conditions for preparative applications are given for the **A*m***/BP/**D*n*** ($m = 1, 3, 5$, $n = 1-3$) systems. The appropriate concentrations of protic solvents such as methanol or water for nucleophilic trapping of radical cations are verified by the product quantum yields which also reflect the importance of BP.

Acknowledgment. We thank Professor K. Schaffner for his generous support, and Mrs. C. Berling, E. Hüttel, G. Klihm and U. Westhoff and Mr. L. J. Currell for technical assistance.

References and Notes

(1) Hoffmann, U.; Gao, Y.; Pandey, B.; Klinge, S.; Warzecha, K.-D.; Krüger, C.; Roth, H. D.; Demuth, M. *J. Am. Chem. Soc.* **1993**, *115*, 10358−10359.
(2) Warzecha, K.-D.; Xing, X.; Demuth, M.; Goddard, R.; Kessler, M.; Krüger, C. *Helv. Chim. Acta* **1995**, *78*, 2065−2076.
(3) Warzecha, K.-D.; Xing, X.; Demuth, M. *Pure Appl. Chem.* **1997**, *69*, 109−112.
(4) Warzecha, K.-D.; Demuth, M.; Görner, H. *J. Chem. Soc., Faraday Trans.* **1997**, *93*, 1523−1530.
(5) Warzecha, K.-D. Ph.D. Thesis, in preparation.
(6) Heinemann, C.; Warzecha, K.-D.; Xing, X.; Demuth, M. *Ind. J. Chem. B* **1997**, *36*, 494−497.
(7) (a) Julliard, M. In *Photoinduced Electron Transfer*; Fox, M. A., Chanon, M., Eds.; Elsevier: Amsterdam, 1988; part B, pp 216−313. (b) Pandey, G. *Top. Curr. Chem.* **1993**, *168*, 175−221. (c) Mattay, J. *Angew. Chem., Int. Ed. Engl.* **1987**, *26*, 825−845. (d) Hinz, S.; Heidbreder, A.; Mattay, J. *Top. Curr. Chem.* **1996**, *177*, 77−124.
(8) Arnold, D. R.; Maroulis, A. J. *J. Am. Chem. Soc.* **1976**, *98*, 5931−5937.
(9) Eriksen, J.; Foote, C. S. *J. Phys. Chem.* **1978**, *82*, 2659−2662.
(10) Spada, L. T.; Foote, C. S. *J. Am. Chem. Soc.* **1980**, *102*, 391−393.
(11) (a) Eriksen, J.; Foote, C. S. *J. Am. Chem. Soc.* **1980**, *102*, 6083−6087. (b) Fujita, M.; Ishida, A.; Majima, T.; Takamuku S. *J. Phys. Chem.* **1996**, *100*, 5382−5387.
(12) Manring, L. E.; Gu, C.-I.; Foote, C. S. *J. Phys. Chem.* **1983**, *87*, 40−44.
(13) Peacock, N. J.; Schuster, G. B. *J. Am. Chem. Soc.* **1983**, *105*, 3632−3638.
(14) Schaap, A. P.; Lopez, L.; Gagnon, S. D. *J. Am. Chem. Soc.* **1983**, *105*, 663−664.
(15) (a) Mizuno, K.; Ichinose, N.; Tamai, T. Otsuji, Y. *Tetrahedron Lett.*, **1985**, *26*, 5823−5826. (b) Mizuno, K.; Tamai, T.; Nakanishi, I.; Ichinose, N.; Otsuji, Y. *Chem. Lett.* **1988**, 2065−2068. (c) Mattes, S. L.; Farid, S. *J. Am. Chem. Soc.* **1986**, *108*, 7356−7361.
(16) Chang, S. L. P.; Schuster, D. I. *J. Phys. Chem.* **1987**, *91*, 3644−3649.
(17) Gassman, P. G.; Bottorff, K. J. *J. Am. Chem. Soc.* **1987**, *109*, 7547−7548.
(18) Gassman, P. G.; De Silva, S. A. *J. Am. Chem. Soc.* **1991**, *113*, 9870−9872.

(19) Lewis, F. D.; Dykstra, R. E.; Gould, I. R.; Farid, S. *J. Phys. Chem.* **1988**, *92*, 7042−7043.
(20) Lewis, F. D.; Bedell, A. M.; Dykstra, R. E.; Elbert, J. E.; Gould, I. R.; Farid, S. *J. Am. Chem. Soc.* **1990**, *112*, 8055−8064.
(21) Gould, I. R.; Ege, D.; Moser, E. J.; Farid, S. *J. Am. Chem. Soc.* **1990**, *112*, 4290−4301.
(22) Todd, W. P.; Dinnocenzo, J. P.; Farid, S.; Goodman, J. L.; Gould, I. R. *J. Am. Chem. Soc.* **1991**, *113*, 3601−3602.
(23) Kikuchi, K.; Hoshi, M.; Niwa, T.; Takahashi, Y.; Miyashi, T. *J. Phys. Chem.* **1991**, *95*, 38−42.
(24) Kanner, R. C.; Foote, C. S. *J. Am. Chem. Soc.* **1992**, *114*, 678−681.
(25) Kanner, R. C.; Foote, C. S. *J. Am. Chem. Soc.* **1992**, *114*, 682−688.
(26) Tsuji, T.; Miura, T.; Sugiura, K.; Matsumoto, Y.; Nishida, S. *J. Am. Chem. Soc.* **1993**, *115*, 482−493.
(27) Kikuchi, K.; Takahashi, Y.; Hoshi, M.; Niwa, T.; Katagiri, T.; Miyashi, T. *J. Phys. Chem.* **1991**, *95*, 2378−2381.
(28) Arnold, D. R.; Snow, M. S. *Can. J. Chem.* **1988**, *66*, 3012−3026.
(29) (a) Arnold, D. R.; Du, X. *Can. J. Chem.* **1994**, *72*, 403−414. (b) Arnold, D. R.; McManus, K. A.; Du, X. *Can. J. Chem.* **1994**, *72*, 415−429. (c) McManus, K. A.; Arnold, D. R. *Can. J. Chem.* **1994**, *72*, 2291−2304. (d) Arnold, D. R.; Du, X.; Chen, J. *Can. J. Chem.* **1995**, *73*, 307−318. (e) Arnold, D. R.; Du, X.; Lijser, H. J. P. *Can. J. Chem.* **1995**, *73*, 522−530. (f) Connor, D. A.; Arnold, D. R.; Bakshi, P. K.; Cameron, T. S. *Can. J. Chem.* **1995**, *73*, 762−771. (g) McManus, K. A.; Arnold, D. R. *Can. J. Chem.* **1995**, *73*, 2158−2169. (h) Arnold, D. R.; Connor, D. A.; McManus, K. A.; Bakshi, P. K.; Cameron, T. S. *Can. J. Chem.* **1996**, *74*, 602−612.
(30) (a) Ohashi, M.; Kudo, H.; Yamada, S. *J. Am. Chem. Soc.* **1979**, *101*, 2201−2202. (b) Kellett, M. A.; Whitten, D. G.; Gould, I. R.; Bergmark, W. R. *J. Am. Chem. Soc.* **1991**, *113*, 358−359. (c) Scurlock, R. D.; Ogilby, P. R. *Photochem. Photobiol.* **1993**, *72*, 1−7. (d) Gould, I. R.; Young, R. H.; Mueller, L. J.; Farid, S. *J. Am. Chem. Soc.* **1994**, *116*, 8176−8187. (e) Gould, I. R.; Moser, J. E.; Armitage, B.; Farid, S. *Res. Chem. Intermed.* **1995**, *21*, 793−806.
(31) (a) Sluggett, G. W.; Turro, N. J.; Roth, H. D. *J. Am. Chem. Soc.* **1995**, *117*, 9982−9989. (b) Weng, H.; Scarlata, C.; Roth, H. D. *J. Am. Chem. Soc.* **1996**, *118*, 10947−10953. (c) Herbertz, T.; Roth, H. D. *J. Am. Chem. Soc.* **1996**, *118*, 10954−10962. (d) Roth, H. D.; Weng, H.; Zhou, D.; Herbertz, T. *Pure Appl. Chem.* **1997**, *69*, 809−814.
(32) Gersdorf, J.; Mattay, J.; Görner, H. *J. Am. Chem. Soc.* **1987**, *109*, 1203−1209.
(33) Görner, H.; Currell, L. J.; Kuhn, H. J. *J. Phys. Chem.* **1991**, *95*, 5518−5523.
(34) Anklam, E.; Asmus, K.-D.; Robertson, L. W. *J. Chem. Soc., Perkin Trans. 2* **1989**, (a) 1569−1572 and (b) 1573−1576.
(35) (a) Arai, S.; Ueda, H.; Firestone, R. F.; Dorfman, L. M. *J. Chem. Phys.* **1969**, *50*, 1072−1077. (b) Dorfman, L. M. *Acc. Chem. Res.* **1970**, *3*, 224−230.
(36) Kato, C.; Hamaguchi, H.; Tasumi, M. *Chem. Phys. Lett.* **1985**, *120*, 183−187.
(37) Sehested, K.; Hart, E. J. *J. Phys. Chem.* **1975**, *79*, 1639−1642.
(38) McClelland, R. A.; Mathivanan, N.; Steenken, S. *J. Am. Chem. Soc.* **1990**, *112*, 4857−4861.
(39) (a) Aloisi, G. G.; Elisei, F.; Görner, H. *J. Phys. Chem.* **1991**, *95*, 4225−4231. (b) Görner, H.; Elisei, F.; Aloisi, G. G. *J. Chem. Soc., Faraday Trans.* **1992**, *88*, 29−34.
(40) (a) Peters, K. S.; Freilich, S. C.; Schaeffer, C. G. *J. Am. Chem. Soc.* **1980**, *102*, 5701−5702. (b) Halpern, A. M.; Forsyth, D. A.; Nosowitz, M. *J. Phys. Chem.* **1986**, *90*, 2677−2679.
(41) (a) Bensasson, R.; Land, E. J. *J. Chem. Soc., Faraday Trans.* **1971**, *67*, 1904−1915. (b) Carmichael, I.; Hug, G. L. *J. Phys. Chem. Ref. Data* **1986**, *15*, 1−250.
(42) Eberson, L.; Hartshorn, M. P.; Persson, O. *J. Chem. Soc., Perkin Trans. 2* **1995**, 1735−1744.
(43) (a) Gschwind, R.; Haselbach. E. *Helv. Chim. Acta* **1979**, *62*, 941−955. (b) Delcourt, M. O.; Rossi, M. J. *J. Phys. Chem.* **1982**, *86*, 3233−3239. (c) Steenken, S.; Warren, C. J.; Gilbert, B. C. *J. Chem. Soc., Perkin Trans. 2* **1990**, 335−342.
(44) Robinson, E. A.; Schulte-Frohlinde, D. *J. Chem. Soc., Faraday Trans. 1* **1973**, 707−718.
(45) Holcman, J.; Sehested, K. *J. Chem. Soc., Faraday Trans. 1* **1975**, 1211−1213.
(46) Kotzenburg, G.; Bastian, E.; Steenken, S. *Angew. Chem., Int. Ed. Engl.* **1988**, *27*, 1066−1067.
(47) Chanon, M.; Eberson, L. In *Photoinduced Electron Transfer*; Fox, M. A., Chanon, M., Eds.; Elsevier: Amsterdam, 1988; part A, pp 409−597.
(48) (a) Rehm, D.; Weller, A. *Isr. J. Chem.* **1970**, *8*, 259−271. (b) Rehm, D.; Weller, A. *Ber. Bunsen-Ges. Phys. Chem.* **1969**, *73*, 834−839.